

Accepted Manuscript

Research papers

Comprehensive drought characteristics analysis based on a nonlinear multivariate drought index

Jie Yang, Jianxia Chang, Yimin Wang, Yunyun Li, Hui Hu, Yutong Chen, Qiang Huang, Jun Yao

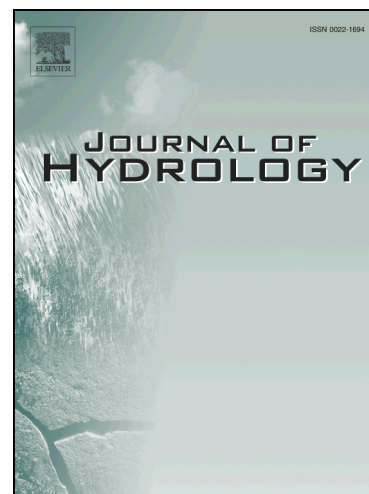
PII: S0022-1694(17)30883-1
DOI: <https://doi.org/10.1016/j.jhydrol.2017.12.055>
Reference: HYDROL 22466

To appear in: *Journal of Hydrology*

Received Date: 24 August 2017
Revised Date: 19 December 2017
Accepted Date: 20 December 2017

Please cite this article as: Yang, J., Chang, J., Wang, Y., Li, Y., Hu, H., Chen, Y., Huang, Q., Yao, J., Comprehensive drought characteristics analysis based on a nonlinear multivariate drought index, *Journal of Hydrology* (2017), doi: <https://doi.org/10.1016/j.jhydrol.2017.12.055>

This is a PDF file of an unedited manuscript that has been accepted for publication. As a service to our customers we are providing this early version of the manuscript. The manuscript will undergo copyediting, typesetting, and review of the resulting proof before it is published in its final form. Please note that during the production process errors may be discovered which could affect the content, and all legal disclaimers that apply to the journal pertain.



Comprehensive drought characteristics analysis based on a nonlinear multivariate drought index

Jie Yang^a, Jianxia Chang^{a,*}, Yimin Wang^a, Yunyun Li^a, Hui Hu^a, Yutong Chen^b, Qiang Huang^a, Jun Yao^c

^aState Key Laboratory Base of Eco-hydraulic Engineering in Arid Area, Xi'an

University of Technology, Xi'an 710048, China

^bPowerChina Guiyang Engineering Corporation Limited, Guizhou Province, Guiyang
550081, China

^cHanjiang - to - Weihe River Valley Water Diversion Project Construction Co. Ltd.,
Shaanxi Province, Xi'an 710048, China

*Correspondence author: chxiang@xaut.edu.cn

Fax: +86-029-82312801

Abstract:

It is vital to identify drought events and to evaluate multivariate drought characteristics based on a composite drought index for better drought risk assessment and sustainable development of water resources. However, most composite drought indices are constructed by the linear combination, principal component analysis and entropy weight method assuming a linear relationship among different drought indices. In this study, the multidimensional copulas function was applied to construct a nonlinear multivariate drought index (NMDI) to solve the complicated and nonlinear relationship due to its dependence structure and flexibility. The NMDI was

constructed by combining meteorological, hydrological, and agricultural variables (precipitation, runoff, and soil moisture) to better reflect the multivariate variables simultaneously. Based on the constructed NMDI and runs theory, drought events for a particular area regarding three drought characteristics: duration, peak, and severity were identified. Finally, multivariate drought risk was analyzed as a tool for providing reliable support in drought decision-making. The results indicate that: (1) multidimensional copulas can effectively solve the complicated and nonlinear relationship among multivariate variables; (2) compared with single and other composite drought indices, the NMDI is slightly more sensitive in capturing recorded drought events; and (3) drought risk shows a spatial variation; out of the five partitions studied, the Jing River Basin as well as the upstream and midstream of the Wei River Basin are characterized by a higher multivariate drought risk. In general, multidimensional copulas provides a reliable way to solve the nonlinear relationship when constructing a comprehensive drought index and evaluating multivariate drought characteristics.

Keywords: Nonlinear multivariate drought index; Multidimensional copulas; Drought events; Drought risk

1. Introduction

Droughts and floods are extreme events (Mishra and Singh, 2010; Hao et al., 2016; Maity et al., 2016) in nature causing great harm to humans, agricultural production and society. They are especially damaging in the northwest arid area of

China (Li et al., 2011; Hao et al., 2016). According to statistics, global economic losses due to droughts reached up to 6-8 billion dollars, far exceeding losses caused by other meteorological disasters (Wilhite, 2001). More seriously, water demand has climbed sharply due to the expanding scale of industry, agriculture, energy, development of the social economy, global warming, and rapid increase of the world's population. It has led to the exacerbation of the water shortage and obvious global drought trend (Cammalleri et al., 2015; Nam et al., 2015; Caracciolo et al., 2016). Therefore, an accurate drought risk assessment is fundamental to prevent and mitigate drought disasters.

Drought event identification is the basis of drought risk assessment. Drought event is a multivariate phenomenon (Xu et al., 2015). Its negative influence presents multivariate drought characteristics (such as drought duration, peak, severity, and affected area). Traditional drought risk assessment only considers one drought characteristic and may not reflect the complex characteristics of drought events (Xu et al., 2015). Therefore, one purpose of this study is the multivariate drought risk assessment considering three drought characteristics: drought duration, peak, and severity.

To accurately identify drought events, a dependable drought index is indispensable. Drought index can reflect drought anomalies or degrees (Wilhite, 2001), and is also the basis for credible drought risk assessment. It is primarily employed to quantify or monitor drought events. Currently, numerous drought indices, including single, multiple, and composite indices (Mishra and Singh, 2010,

Cammalleri et al., 2015; Waseem et al., 2015) have been used to evaluate different types of droughts. A single drought index only considers one variable, such as precipitation, runoff or soil moisture (Waseem et al., 2015). A multiple drought index takes more variables into consideration. A single drought index or multiple drought index mostly can typically reflect one type of drought (meteorological, hydrological, agricultural or socioeconomic drought). In addition, drought events identifications based on different drought indices are a little bit different from each other. Most importantly, different types of droughts may occur simultaneously, and it is hard to distinguish them (Hao and Singh, 2015). Therefore, the single and multiple drought indices are insufficient to reveal the complicated relationship among different variables. To overcome this issue, the composite index was proposed.

A composite index entails constructing an index based on different drought indices (Rajsekhar et al., 2015) which can reflect multivariate drought variables simultaneously (Huang et al., 2015; Chang et al., 2016). There have been numerous studies that have focused on constructing a composite index based on different methods. Linear combination is a candidate to combine different drought indices. Svoboda et al. (2002) proposed an Objective Blend of Drought Indicators (OBDI) based on a linear weighted method. A linearly combined drought index (LDI) assuming the same weight was employed to predict the drought by Hao et al. (2016). The principal component analysis (PCA) is another way to construct the multivariate drought index. Meyer et al. (1991) proposed to use the PCA to combine the PDSI with Crop Moisture Index (CMI). Keyantash and Dracup (2004) developed an aggregate

drought index (ADI) that integrates meteorological, hydrological and agricultural droughts based on PCA. Entropy theory is also a mean to construct the composite drought index. A multivariate drought index (MDI) was built by Rajsekhar et al. (2015) based on entropy method. Waseem et al. (2015), Huang et al. (2015) and Chang et al. (2016) also built composite drought indices using this method.

Composite drought indices constructed by the linear combination, principal component analysis, and entropy weight method all assume a linear relationship among different drought indices (Mo and Lettenmaier, 2014). Therefore, some researchers proposed to employ the copulas function to solve the complicated and nonlinear relationship among multiple variables (Kao and Govindaraju, 2010; Hao and AghaKouchak, 2013; Ma et al., 2014). The copulas function is a method which has been widely used in hydrological fields such as multivariate drought frequency analysis (Huang et al., 2014; Xu et al., 2015) and hydrometeorological extremes (Kao and Govindaraju, 2010). Copulas is a flexible statistical tool which can be used to construct the joint distribution function by combining multiple univariate marginal distribution functions according to the dependence structure (Hao and Singh, 2015). There is no limitation in choosing the marginal distribution function of univariate drought index, i.e. margin-free characteristics (Favre et al., 2004). In addition, all margin-free characteristics can be fully maintained (Jeong and Lee, 2015). More importantly, there are a set of copulas families that can describe the nonlinear, symmetric, or asymmetric relationship. A copula-based joint deficit index (JDI) was constructed by Kao and Govindaraju (2010) based on precipitation and streamflow.

Hao and AghaKouchak (2013) put forward a Multivariate Standardized Drought Index (MSDI) based on 2-dimensional copulas to reflect meteorological and agricultural droughts at the same time. The copulas function can also be employed to higher dimensions to characterize multiple drought types at the same time. Ma et al. (2014) put forward the Standardized Palmer Drought Index (SPDI)-based Joint Drought Index (SPDI-JDI) based on multidimensional copulas function. These studies prove the effectiveness and feasibility of using copulas to construct a composite drought index. Nonetheless, since the research on the construction of the composite drought index based on multidimensional copulas function is still limited, another purpose of this study is to construct a nonlinear multivariate drought index (NMDI) based on multidimensional copulas function to simultaneously reflect meteorological, hydrological and agricultural drought variables (precipitation, runoff, and soil moisture).

The Wei River Basin is one of the most important grain and industrial production bases in China. It plays an important role in the Western China's Development. Nevertheless, due to the impacts of climate change and human activities, runoff has decreased (Yang et al., 2016). At the same time, with the development of the economy, water demand is growing each year. Therefore, there is an imbalance between water supply and water demand, leading to frequent droughts. A more accurate assessment of drought risk in the Wei River Basin can aid in the planning and sustainable development of water resources, drought early warning and relief.

The Wei River Basin was chosen as the study area because of this challenging

problem. As a reliable drought index is the basis of drought risk assessment, the main purposes of this study are (1) to construct a reliable nonlinear multivariate drought index (NMDI), and (2) to conduct a multivariate drought risk assessment considering three drought characteristics: duration, peak and severity for early drought warning and mitigation.

2. Study area and data sources

The Wei River is the largest tributary of the Yellow River at 818 km in length. The average slope of the main stream is 0.223%. It flows through Gansu, Ningxia and Shaanxi provinces, covering about 134,800 km² and accounting for 18% of the area of the Yellow River Basin (Chang et al., 2016). It is located at 104°E-110.4°E, 33°N-38°N in an arid and semi-arid region. The mean annual rainfall of the Wei River Basin is about 527 mm and much higher in the south (over 800mm) than the north (lower than 550mm). The largest monthly rainfall mainly occurs in July or August whereas the minimum occurs in December or January. Rainfall from July to October accounts for over 60% of the annual rainfall (Huang et al., 2014). The mean annual evaporation ranges from approximately 600-1600 mm. The mean annual runoff is approximately 100.4×10^8 m³, comprising 17.3% of the runoff in the Yellow River.

The Wei River Basin (WRB) is divided into five partitions: the Jing River Basin (JRB), Beiluo River Basin (BRB), upstream of the Wei River Basin (UWRB), midstream of the Wei River Basin (MWRB), downstream of the Wei River Basin (DWRB) (illustrated in Fig. 1). The precipitation, average vapor pressure, average air

temperature, minimum and maximum air temperature, average sunshine hours, and average wind speed of 21 meteorological stations in the Wei River Basin were gathered from the National Climate Center of the China Meteorological Administration and are shown in Fig. 1. The runoff in the JRB, BRB, UWRB, MWRB, and LWRB were collected from 5 hydrological stations (Zhangjiacun, Zhuangtou, Linjiacun, Xianyang and Huanxian) based on data published by the hydrology bureau of the Yellow River Conservancy Commission. Soil types were obtained from the World Soil Information. The data period is from 1960 to 2005. The meteorological data of the JRB, BRB, UWRB, MWRB, LWRB and WRB were calculated using the Thiessen polygon method.

Fig. 1. Meteorological stations and hydrological stations in the Wei River Basin

3. Methodology

The main flowchart used to construct the nonlinear multivariate drought index (NMDI) and to assess multivariate drought risk (the two purposes of this study) is displayed in Fig. 2. The detailed calculations are to follow.

Fig. 2. Main flowchart of construction of the NMDI and drought risk assessment

3.1. Nonlinear multivariate drought index (NMDI)

Due to the complicated and nonlinear relationship among different drought indices, the multidimensional copulas function was employed in this study to construct a nonlinear multivariate drought index (NMDI) by integrating

meteorological, hydrological, and agricultural drought indices according to its margin-free characteristics and structure dependence (Kao and Govindaraju, 2010).

There are three steps to construct the NMDI.

Step 1: Calculation of the monthly meteorological, hydrological and agricultural drought indices values.

Step 2: Selection of the optimal marginal distribution functions of monthly meteorological, hydrological, and agricultural drought indices values.

Step 3: Selection of the optimal copulas function to construct the NMDI.

3.1.1 Three drought indices

Precipitation anomaly percentage (PAP), streamflow drought index (SDI), and modified palmer drought severity index (MPDSI) were employed as the meteorological, hydrological and agricultural drought index, respectively. Time scales for PAP, SDI, and MPDSI are all one month in this study; therefore, the time scale of the constructed NMDI is also one month.

The PAP can directly reflect a drought caused by a precipitation anomaly. The method is simple, and the data required is easy to obtain. Therefore, it has been widely used (Chang et al., 2016). The formula for PAP is defined as follows:

$$PAP = \frac{P - \bar{P}}{\bar{P}} \quad (1)$$

where P is the monthly precipitation; and \bar{P} is the average monthly precipitation.

The calculation of SDI is simple, stable and flexible. In addition, it can reflect

the intensity and duration of a drought. Hence, it has been widely applied (Nalbantis and Tsakiris, 2009; Tabari et al., 2013). The formula of the SDI is as follows:

$$Z = SDI = S \frac{t - (c_2 t + c_1)t + c_0}{((d_3 t + d_2)t + d_1)t + 1.0} \quad (2)$$

where $t = \sqrt{\ln \frac{1}{F^2}}$; if $F > 0.5$, $S = 1$; Conversely, if $F \leq 0.5$, $S = -1$;

$F(x < x_0) = \int_0^{\infty} f(x) dx$; x is the measured monthly runoff; $F(x < x_0)$ is the cumulative probability function of the measured runoff; $f(x)$ is the probability density function of the measured runoff; and $f(x)$ obeys the gamma distribution; $c_0 = 2.515517$, $c_1 = 0.802853$, $c_2 = 0.010328$, $d_1 = 1.432788$, $d_2 = 0.189269$, and $d_3 = 0.001308$.

The PDSI was proposed by Palmer (1965) based on the water balance equation. This index considers the previous precipitation, water supply and water demand, and can provide clear physical description as it nicely captures the variation of soil moisture. Currently, it is the most widely used drought index (Ma et al., 2013; Nam et al., 2015). The PDSI was constructed according to data from the United States. It is not sensitive in the northwest of China (Chang et al., 2016). Therefore, it must be modified to accurately identify a drought event. The formula of the modified PDSI (MPDSI) (Chang et al., 2016) in the Wei River Basin is expressed as follows:

$$MPDSI = X_i = Z_i / 216 + 0.9213X_{i-1} \quad (3)$$

where X_i is the drought index; Z_i denotes the abnormal moisture index.

$$Z = dK \quad (4)$$

$$d = P - \hat{P} \quad (5)$$

$$K_i = \frac{2601.3}{\sum_{j=1}^{12} \bar{D}_j K'_j} K' \quad (6)$$

$$K' = 4.3208 \log_{10} \left(\frac{\overline{PE}_i + \bar{R}_i + \overline{RO}_i}{(\bar{P}_i + \bar{L}_i) \bar{D}_i} \right) + 8.9661 \quad (7)$$

where K_i is the climatic characteristic coefficient; K' is the modified climatic characteristic coefficient; d represents the difference between P (measured monthly precipitation); and \hat{P} (monthly precipitation in suitable climate condition). \overline{PE} , \bar{R} , \overline{RO} , \bar{P} , \bar{L} , \bar{D} refer to average potential evapotranspiration, average water supplement, average runoff, average precipitation, average water loss, and average absolute value of d .

Drought grade classifications of meteorological, hydrological, and agricultural drought indices are shown in Table 1.

Table 1 Drought grade classifications of the PAP, SDI, and MPDSI

3.1.2 Selection of the optimal marginal distribution functions of three drought indices

To better preserve all margin-free characteristics (Jeong and Lee, 2015), in this paper, a larger set of marginal distribution functions including Gamma, Rayleigh, Log-normal, Normal, Beta, Exponential, Weibull, and Generalized pareto were selected as candidates to fit the monthly PAP, SDI, and MPDSI values (shown in Table 2).

As the monthly PAP, SDI, and MPDSI had negative values, some marginal distribution functions were not applicable. Therefore, normalization was conducted (Madadgar et al., 2014) to ensure that three monthly drought indices values were all in

the interval of [0, 1]. Then, parameters of these eight marginal distribution functions for three normalized drought indices values were estimated based on the maximum likelihood algorithm.

Table 2 Probability density functions of eight marginal distribution functions

For each drought index, there are eight marginal distribution functions. An optimal marginal distribution function of each drought index must be chosen to better represent the properties of each drought index in this region. The optimal marginal distribution functions of three drought indices values were selected with the highest goodness-of-fit (GOF), i.e. the lowest values of three evaluation indices: the root mean square error (*RMSE*), ordinary least squares (*OLS*) and Akaike information criteria (*AIC*) (Akaike, 1974). *RMSE*, *OLS* and *AIC* are computed as follows:

$$P_e = P(A \leq a_i) = \frac{\sum_{m=1}^i N_m - 0.44}{n + 0.12} \quad (8)$$

$$MSE = \frac{1}{n-1} \sum_{i=1}^n (P_e - P_t)^2 \quad (9)$$

$$OLS = \sqrt{\frac{1}{n} \sum_{i=1}^n (P_e - P_t)^2} \quad (10)$$

$$RMSE = \sqrt{MSE} \quad (11)$$

$$AIC = n \log(MSE) + 2k \quad (12)$$

where P_e is the empirical cumulative probability of monthly PAP, SDI, or MPDSI values; N_m represents the number counted as $A \leq a_i$; n is the total number; P_t is the theoretical cumulative probability of monthly PAP, SDI, or MPDSI values calculated based on the determined optimal parameters; and k is the total number of the function

parameters.

3.1.3 Construction of the Nonlinear multivariate drought index (NMDI)

In this study, four families belonging to 3-dimensional Archimedean copulas: Gumbel-Hougaard (Gumbel), Ali-Mikhail-Haq (AMH), Clayton and Frank were chosen as the candidates to construct the nonlinear multivariate drought index (NMDI). Distribution functions of four multidimensional Archimedean copulas are listed in Table 3.

Table 3 Distribution functions of multidimensional Archimedean copulas

In this study, the curve-fitting method (Zhang and Song, 2011) was used to determine the optimal parameters of four copulas with the highest goodness-of-fit by comparing the 3-dimensional theoretical joint cumulative probability of three drought indices: PAP, SDI, and MPDSI and 3-dimensional empirical joint cumulative probability of three drought indices: PAP, SDI, and MPDSI (Eq. (13)).

$$H(a,b,c) = P(A \leq a_i, B \leq b_i, C \leq c_i) = \frac{\sum_{m=1}^i \sum_{l=1}^i \sum_{k=1}^i N_{mlk} - 0.44}{n + 0.12} \quad (13)$$

where $H(a,b,c)$ is the 3-dimensional empirical joint cumulative probability of three drought indices: PAP, SDI, and MPDSI; N_{mlk} represents the number counted as $A \leq a_i, B \leq b_i, C \leq c_i$; n is the total number.

Assuming that the theoretical cumulative probabilities of PAP, SDI, and MPDSI are $F(X)$, $G(Y)$ and $K(Z)$ (simplified as u, v, w), respectively. The formula of the NMDI drought index can be calculated based on the 3-dimensional theoretical joint

cumulative probability of three drought indices: PAP, SDI, and MPDSI, which is defined as follows (Madadgar et al., 2014).

$$NMDI=C[F(X),G(Y),K(Z)]=C[u,v,w] \quad (14)$$

where C is the copulas joint distribution function; $C[u,v,w]$ is the 3-dimensional theoretical joint cumulative probability of three drought indices.

As four families of copulas functions all have their own best goodness-of-fit, therefore, the optimal copulas function must be determined to construct a more reasonable drought index. The best copulas function was determined by analyzing which copulas function has the highest goodness-of-fit. After selection of the optimal copulas, the formula to calculate the NMDI (Eq. (14)) was obtained based on the corresponding copulas joint distribution function and optimal parameters of the optimal copulas (Table 3). Next, the monthly NMDI values was computed based on the formula and the optimal theoretical cumulative probabilities of PAP, SDI, and MPDSI. Then, the drought grade classifications of the NMDI was acquired based on the normalized drought grade classifications of PAP, SDI, and MPDSI and the formula of the NMDI.

3.2. Drought risk assessment

3.2.1 Identification of drought events

To assess the drought risk, it is necessary to identify drought events, including three drought characteristics: the drought duration (D), severity (S) and peak (P) based on the runs theory (Cancelliere and Salas, 2004; Chang et al., 2016).

In this study, the drought event is defined as the constructed NMDI values smaller than the truncation level (the critical value between the no drought and slight drought). Duration (D) is the number of continuous months of the drought event (the months when NMDI values are smaller than the critical value). Drought severity (S) is the cumulative deficit below the critical value of the drought event. Drought peak (P) is the maximal gap between the NMDI value and the critical value of the drought event.

3.2.2 Drought risk assessment

In this study, drought risk is defined as the likely occurrence drought possibility for a given duration, peak and severity. The multivariate drought risk can be derived as follows:

$$P(D \geq d \cap P \geq p \cap S \geq s) = 1 - u - v - w + c[u, v] + c[u, w] + c[w, v] - c[u, v, w] \quad (15)$$

where $P(D \geq d \cap P \geq p \cap S \geq s)$ is the multivariate drought risk (joint exceedance possibility). $c[u, v]$, $c[u, w]$ and $c[w, v]$ are the 2-dimensional joint cumulative probability of duration and peak, duration and severity, peak and severity, respectively. The calculation of optimal marginal distribution functions of drought duration, peak, and severity and the optimal copulas function to derive the joint distribution of three characteristics are similar with that in Section 3.1.2 and Section 3.1.3, respectively.

4. Results and discussions

4.1. Marginal distribution of the calculated PAP, SDI, and MPDSI values

Based on the description in Section 3.1, the foundation work to construct the NMDI is to calculate the monthly PAP, SDI, and MPDSI values and to determine their corresponding optimal marginal distribution functions.

Monthly PAP, SDI, and MPDSI values in the five partitions, as well as the whole Wei River Basin, were calculated based on the formulas in Section 3.1.1. Next, eight marginal distribution functions were employed to fit the normalized monthly PAP, SDI, and MPDSI values in the five partitions and the whole Wei River Basin. Then, the optimal parameters of eight marginal distribution functions for PAP, SDI, and MPDSI values in five partitions and the whole Wei River Basin were estimated based on the maximum likelihood algorithm. Afterwards, the optimal goodness-of-fit (GOF) of eight marginal distribution functions was calculated by comparing the theoretical cumulative probability of PAP, SDI, or MPDSI (calculated based on optimal marginal distribution function parameters) and the empirical cumulative probability of PAP, SDI, or MPDSI (Eq. (8)). The GOF criteria results of eight distribution functions and their corresponding parameters for the PAP in the JRB were taken as an example and listed in Table 4.

Table 4 GOF criteria results of the marginal distribution functions and parameters of the PAP in the JRB

The smallest are the three evaluation indices, and the goodness-of-fit of the selected marginal distribution function is the best. Table 4 shows that for the monthly PAP values in the JRB, three evaluation indices of Weibull are smallest with

$RMSE=0.0310$, $OLS=0.0309$, and $AIC=-1625.81$. Therefore, Weibull with $\alpha =0.2242$, $\beta =1.3716$ is the most appropriate marginal distribution function to fit the monthly PAP values in the JRB.

Similarly, in the JRB, the Weibull and Normal marginal distribution functions are optimal for the monthly SDI and MPDSI values, respectively. Weibull, Normal, and Normal fit the monthly PAP, SDI, and MPDSI values in the BRB best, respectively. Weibull, Weibull, and Normal are most appropriate to fit the monthly PAP, SDI, and MPDSI values in the UWRB, respectively. The best fit marginal distribution functions of the monthly PAP, SDI, and MPDSI values in the MWRB are Weibull, Normal, and Normal, respectively. The optimal marginal distribution functions of the monthly PAP, SDI, and MPDSI values in the LWRB are Weibull, Weibull, and Normal, respectively. Weibull, Weibull, and Normal fit the monthly PAP, SDI, and MPDSI values in the WRB best, respectively.

4.2. Construction of the nonlinear multivariate drought index

After determining the optimal marginal distribution functions and their parameters of monthly PAP, SDI, and MPDSI values, four families of 3-dimensional Archimedean copulas: Gumbel, AMH, Clayton and Frank were employed to construct the NMDI in the five partitions and the whole Wei River Basin.

For each copulas function, when the 3-dimensional theoretical joint cumulative probability of three drought indices: PAP, SDI, and MPDSI is nearest to the 3-dimensional empirical joint cumulative probability of three drought indices (Eq. (13))

based on lowest values of three evaluation indices (*RMSE*, *OLS* and *AIC*), the parameter of the copulas function is the best.

In this study, the curve-fitting method was applied to derive the optimal parameter of the Gumbel, AMH, Clayton and Frank. The GOF criteria results from the four copulas functions and their corresponding optimal parameters in the five partitions and the whole Wei River Basin are shown in Table 5.

Table 5 GOF criteria results of the optimal Archimedean copulas and parameters in the five partitions and the WRB

Table 5 shows that in the JRB, three evaluation indices of Gumbel are lowest with $RMSE=0.053936$, $OLS=0.053886$, and $AIC=-1367.57$, revealing that the Gumbel copula with parameter $\theta=1.3674$ is the best function to construct the NMDI according to the optimal marginal distributions of PAP, SDI, and MPDSI. Similarly, the Gumbel copula was also used for the MWRB, LWRB, and WRB while the Frank copula was used for BRB and UWRB.

Based on the corresponding parameters, distribution functions of the optimal copulas function, and the optimal theoretical cumulative probabilities of PAP, SDI, and MPDSI, monthly NMDI values (3-dimensional theoretical joint cumulative probability of three drought indices) in the five partitions and the whole Wei River Basin were obtained. The comparisons between the 3-dimensional empirical and optimal theoretical joint cumulative probability of three drought indices are shown in Fig. 3.

Fig. 3. Comparisons between 3-dimensional empirical and theoretical joint

cumulative probability of three drought indices

Fig. 3 shows that the 3-dimensional theoretical joint cumulative probability of three drought indices is quite close to the 3-dimensional empirical joint cumulative probability of three drought indices in the five partitions and the WRB. This result illustrates the reliability of the selected optimal Archimedean copulas and optimal parameters.

The drought grade classifications of the NMDI must be determined to better assess the drought degrees. Taking the JRB as an example, based on the selected optimal copulas Gumbel (Table 5), its optimal parameter, and the normalized drought grade classifications of PAP, SDI, and MPDSI (Table 1), the drought grade classifications of the NMDI in the JRB were calculated according to Eq. (14). Similarly, drought grade classifications of the NMDI in the BRB, UWRB, MWRB, LWRB, and the whole WRB were obtained as shown in Table 6. The spatial diagram of the drought grade classifications is shown in Fig. 4.

Table 6 Drought grade classifications of the NMDI

Fig. 4. Spatial diagram of drought grade classifications of NMDI

Above the blue isosurface, there is no drought. The space between the blue and green isosurface represents slight droughts. The space between the green and yellow isosurface represents moderate droughts. The space between the yellow and red isosurface is severe drought and finally, the space below the red isosurface is extreme drought.

4.3. Comparison between the NMDI and other drought indices

To verify the reliability of the constructed NMDI, in this study, taking the NMDI, PAP, SDI, and MPDSI values of the WRB in 2000 as an example, the comparison was plotted in Fig. 5 for better visualization.

Fig. 5. Comparison between the NMDI, PAP, SDI, and MPDSI of the WRB in 2000.

Fig. 5 shows that the variation trend of the monthly NMDI values is relatively consistent with the variation trends of the monthly PAP, SDI, and MPDSI values. The increase or decline of the PAP, SDI, and MPDSI values will also lead to a corresponding increase or decline of the NMDI values.

As the NMDI was constructed based on the PAP, SDI, and MPDSI, it should reflect the multiple (meteorological, hydrological and agricultural) drought properties. The correlation analyses between two drought indices are shown in Table 7.

Table 7 Correlation analyses among different drought indices

Table 7 shows that the correlations between two single drought indices (PAP-SDI, PAP-MPDSI and SDI-MPDSI) are generally around 0.4, and the correlations between the constructed composite drought index NMDI and single drought index (PAP-NMDI, SDI-NMDI and MPDSI-NMDI) typically exceed 0.7. The correlations between two single drought indices are obviously smaller than the correlations between the constructed composite drought index NMDI and single drought index. This indicates that to some extent, the meteorological drought index (PAP) cannot reflect the hydrological and agricultural droughts very well. Similarly, the hydrological drought index (SDI) cannot reflect the meteorological and agricultural

droughts very well, and the agricultural drought index (MPDSI) cannot assess the meteorological and hydrological drought very well. However, the constructed nonlinear multivariate drought index (NMDI) can relatively reflect the multiple (meteorological, hydrological and agricultural) drought properties better. The constructed NMDI provides a new perspective to reflect meteorological, hydrological and agricultural drought properties at the same time.

To further prove the reliability of the constructed NMDI, a drought frequency comparison analysis between the constructed NMDI and other single or composite drought index proposed in this study area (PAP, SDI, MPDSI, and MIDI) is essential (shown in Fig. 6). In this study, drought frequency means the occurrence possibility of different grades of droughts.

Fig. 6. Drought frequency comparison analysis among the different drought indices

Fig. 6 shows that, for the yearly total droughts, the drought frequency in the JRB is the highest based on the NMDI. This is in agreement with the values calculated by the MPDSI and MIDI. The frequency of slight droughts is the highest in the BRB based on the NMDI, which is consistent with results from the SDI, MPDSI and MIDI. The frequency of moderate droughts in the UWRB is higher than others based on the NMDI, which is in agreement with those computed by the SDI, MPDSI, and MIDI. The frequencies of severe droughts are the highest in the JRB, UWRB and MWRB, which is also unanimous with the frequencies calculated by the SDI, MPDSI, and MIDI. The frequency of extreme drought is the highest in the JRB based on the NMDI, which is similar to the PAP, MPDSI, and MIDI results, as well. The yearly

drought frequency analysis based on the NMDI is relatively consistent with the PAP, SDI, MPDSI, and MIDI, indicating that the drought frequency analysis based on the NMDI is reliable. Fig. 6 also shows that drought frequencies in the JRB, UWRB and MWRB are relatively higher.

As the yearly drought properties may cover the seasonal drought properties, the seasonal drought frequency based on the NMDI was also calculated shown in Fig. 7. Spring drought is defined as a drought that occurred from March to May. Summer drought is from June to August. Autumn drought is from September to November. Winter drought is from December to next February.

Fig. 7. Seasonal drought frequency analysis based on the constructed NMDI

Fig. 7 shows that the frequencies of the total spring droughts are the highest in the JRB and UWRB. For total summer droughts, the frequency is the highest in the MWRB. The frequency of the total autumn droughts is the highest in the UWRB. The frequencies of the total winter droughts are the highest in the JRB and MWRB. A slight spring, summer, autumn, and winter droughts are likely to occur in the BRB, MWRB, BRB, and JRB, respectively. The frequencies of moderate spring, summer, autumn and winter droughts in the JRB, MWRB, UWRB, and UWRB are the highest, respectively. The frequencies of severe spring, summer, autumn and winter droughts in the UWRB, JRB, MWRB and MWRB are the highest, respectively. The frequencies of extreme spring, summer, autumn, and winter droughts in the JRB, MWRB, JRB, and JRB are the highest.

Based on Fig. 6 and Fig. 7, we conclude that the drought frequency in the JRB is

relatively the highest followed by the MWRB and UWRB. In addition, drought frequency analysis is consistent with other research (Huang et al., 2015; Chang et al., 2016), indicating that the constructed NMDI is reliable.

To further prove the behavior and reliability of the NMDI, whether the constructed NMDI could snap a historical drought was also analyzed. In this study, five years (1978, 1980, 1995, 1997 and 2000) were selected that had recorded severe or extreme drought occurrences (Wang et al., 2013; Chang et al., 2016). The comparisons of whether PAP, SDI, MPDSI, MIDI and NMDI could snap these droughts are shown in Table 8.

Table 8 Captured drought events based on the PAP, SDI, MPDSI, MIDI, and NMDI

Table 8 shows that the constructed NMDI basically captures more recorded severe or extreme drought occurrences than the PAP, SDI, MPDSI and MIDI. That indicates the NMDI can better reflect the complex multivariate natural variables.

Among these five drought indices, the fewest amount of droughts are captured based on the PAP. The reason may be that the PAP only considers one variable: precipitation, rather than multivariate variables.

Based on the outlined above, the constructed nonlinear multivariate drought index (NMDI) has a good reliability and it can identify multivariate drought types (meteorological, hydrological and agricultural droughts) at the same time. In addition, it can basically capture more recorded drought occurrences indicating that the NMDI provides a fuller picture than other drought indices.

4.4. Multivariate analysis of the drought risk

Based on the runs theory in Section 3.2, drought events regarding three drought characteristics: the drought duration (D), drought peak (P) and drought severity (S) were identified based on the NMDI in the five partitions and the WRB as a whole.

There were 90, 98, 80, 83, 85, and 83 drought events in the JRB, BRB, UWRB, MWRB, LWRB, and WRB, respectively. The drought peak, severity and duration of these drought events in five partitions are shown in Table 9.

Table 9 Drought peak, severity, and duration corresponding to drought events

Table 9 shows that the maximum drought duration in the BRB is the shortest at 8 months, and that the maximum drought severity of 0.79 is relatively smaller than those in other partitions, indicating that droughts in the BRB are relatively less serious. However, the maximum drought duration in the MWRB is the longest: 17 months, while the maximum drought peak of 0.1 is relatively higher and maximum drought severity of 1.5 is the highest, showing that droughts in the MWRB are very serious. Droughts in the UWRB and JRB are also very serious. On the whole, drought in the Wei River Basin is a significant issue.

To better analyze the drought risk regarding three drought characteristics: duration, peak, and severity to better plan and manage water resources, alleviate the drought and develop drought warning systems, the four families of 3-dimensional copulas function were also employed to inquire into the multivariate drought risk, i.e., the joint exceedance possibility.

First, it was necessary to derive the optimal marginal distribution functions of the

duration, peak and severity based on eight marginal distribution functions in the five partitions and the WRB. The calculation method is similar with that shown in Table 4.

The results show that the optimal marginal distribution functions for the duration, severity, and peak in the JRB are Rayleigh, Beta, and Normal, respectively. Rayleigh, Gamma, and Generalized pareto fit the duration, severity, and peak in the BRB best, respectively. Rayleigh, Gamma, and Generalized pareto are most appropriate to fit duration, severity, and peak in the UWRB, respectively. The best fit marginal distribution functions of the duration, severity, and peak in the MWRB are Rayleigh, Log-normal, and Normal, respectively. The optimal marginal distribution functions for the duration, severity, and peak in the LWRB are Rayleigh, Log-normal, and Generalized pareto, respectively. In the WRB, Rayleigh, Generalized pareto, and Generalized pareto fit the duration, severity, and peak best, respectively.

After confirming the optimal marginal distribution functions and parameters of the drought duration, peak and severity, four families of 3-dimensional Archimedean copulas (including Gumbel, AMH, Clayton, and Frank) were employed to derive the multivariate drought risk. The calculation process is similar with that in Section 4.2.

The GOF criteria results of four copulas functions and their corresponding optimal parameters to derive the multivariate drought risk in the five partitions and the whole Wei River Basin, are shown in Table 10

Table 10 GOF criteria results of the optimal 3-dimensional copulas and parameters for drought D , P , and S

Table 10 shows that in the JRB, three evaluation indices of the Gumbel are

lowest with $RMSE=0.0718$, $OLS=0.0714$, and $AIC=-203.8990$, showing that the Gumbel with parameter $\theta=3.1731$ is best to construct the joint distribution of three drought characteristics: the duration, peak and severity. Similarly, optimal 3-dimensional Archimedean copulas functions used to construct the joint distribution of three drought characteristics are Frank, Frank, Gumbel, Frank and Frank in the BRB, UWRB, MWRB, LWRB, and WRB, respectively.

Next, the multivariate drought risks in the five partitions and the whole Wei River Basin were calculated based on Eq. (15), optimal marginal distribution functions of three drought characteristics, optimal copulas functions and its optimal parameters (shown in Table 10). The multivariate slice map of the drought risk is shown in Fig. 8. The multivariate isosurfaces of the drought risk are shown in Fig. 9.

Fig. 8. Slice map of multivariate drought risk

Fig. 8 is used to analyze how the multivariate drought risk reacts to the variation of the drought duration, peak and severity. Fig. 8 shows the slice map of multivariate drought risk under the conditions $pd=0.25$, $pd=0.5$, $pd=0.75$, $pp=0.25$, $pp=0.5$, $pp=0.75$, $ps=0.25$, $ps=0.5$ and $ps=0.75$ (pd , pp , and ps are the theoretical cumulative probability of the drought duration, peak and severity, respectively). The higher the ps is, the greater the drought severity. The higher the pd is, the longer the drought duration. The higher the pp is, the greater the drought peak. The color represents the multivariate drought risk possibility values.

Fig. 8 shows that the law of drought risk in the five partitions and the WRB is similar. Taking the JRB as an example, and keeping the pd and pp constant (for

example when $pd=0.25$ and $pp=0$), the higher the ps is, the lower the multivariate drought risk. Similarly, with the increase of pd or the pp , multivariate drought risk declines. The multivariate drought risk negatively correlated with the cumulative probability of the duration, peak and severity. This result indicates that the more severe the drought, the lower the multivariate drought risk. It also indicates that the more serious the duration, peak and severity, the less likely is the occurrence of a corresponding drought event.

Fig. 9. Contour surface of the multivariate drought risk of the D , P and S

Fig. 9 shows the multivariate isosurfaces when $pre=0.1$ (pre is the 3-dimensional i.e. multivariate drought risk possibility), $pre=0.2$, $pre=0.3$, $pre=0.4$, $pre=0.5$, $pre=0.6$, $pre=0.7$, $pre=0.8$ and $pre=0.9$. It shows the isosurfaces of multivariate drought risk from the viewing angle. It also illustrates that when cumulative probability of duration, peak and severity increases, the multivariate drought risk declines, which agrees with Fig. 8. It also indicates that the likely occurrence drought possibility of severe or extreme droughts is lower than that of light droughts. Therefore, in practice, more attention should be paid to the slight or moderate drought events.

In this study, multivariate drought risks under two scenarios (scenario 1: droughts more likely to happen $P(D \geq 2 \cap P \geq 0.05 \cap S \geq 0.05)$; scenario 2: droughts less likely to happen $P(D \geq 4 \cap P \geq 0.075 \cap S \geq 0.1)$) in the five partitions are demonstrated in Fig. 10.

Fig. 10. Drought risks under two scenarios

Fig. 10 shows that for scenario 1, the multivariate drought risks in the JRB,

UWRB, MWRB, BRB, and LWRB are 0.59, 0.68, 0.65, 0.50, and 0.48, respectively.

For scenario 2, the multivariate drought risks in the JRB, UWRB, MWRB, BRB, and LWRB are 0.10, 0.24, 0.30, 0.14, and 0.12, respectively. The likely occurrence drought possibilities of scenario 1 in the JRB, UWRB, and MWRB are higher than those in the other partitions. The likely occurrence drought possibilities of scenario 2 in the UWRB and MWRB are higher than those in the other partitions. The multivariate drought risks in the UWRB, MWRB, and JRB are relatively higher than those in the other partitions. This indicates that for a given duration, peak, and severity, the likely occurrence drought possibilities in the JRB, UWRB, and MWRB are higher.

This result is in accordance with the drought frequency analysis based on the NMDI in Fig. 6 and Fig. 7. The reason why the drought frequency and multivariate drought risk in the JRB, UWRB, and MWRB are shown as follows. From the angle of the terrain, the geomorphology in the JRB is mainly loess. The soil texture is relatively coarse, and the vegetation is rare, leading to poor water retention. Moreover, the JRB is the main source of the sediment of the Yellow River; the soil and water losses in the JRB are the most serious in the Wei River Basin. With regards to climate, precipitation is mainly concentrated in summer, and it is not easy to store. In addition, evapotranspiration is larger due to abundant sunshine. Therefore, the capacity to resist drought in the JRB is low. Many important cities such as Xi'an, Xianyang and Tianshui, are located in UWRB and MWRB, and many studies have stated that due to human activities and climate variation, runoff in these cities has markedly declined (Chang et al., 2014; Chang et al., 2016). More importantly, the increasing number of

people moving to these cities has resulted in a sharp increase of water demand. At the same time, evaporation has increased due to the rising temperature. These factors all lead to the higher drought risks in the UWRB and MWRB. The Wei River Basin is facing a serious drought risk which will compromise the basin's sustainable development. Therefore, relevant government departments should take greater measures regarding early drought warning and drought relief to better prevent and control the droughts.

5. Conclusions

Previous research mainly focused on constructing the composite drought index to analyze multivariate drought characteristics based on the linear combination, principal component analysis, and entropy weight method assuming a linear relationship among different drought indices. In this study, a nonlinear multivariate drought index (NMDI) was constructed based on the multidimensional Archimedean copulas. Then, based on the constructed NMDI and runs theory, drought events regarding three drought characteristics: drought duration, peak and severity were identified. Multivariate drought risks were also assessed in the Wei River Basin for better drought early warning and relief. The main conclusions are as follows:

(1) The NMDI was constructed to derive the joint distribution of three drought indices: PAP, SDI, and MPDSI based on their optimal marginal distribution functions and the NMDI formula. The NMDI formula was computed according to the optimal parameters and corresponding joint distribution function of the optimal copulas.

Results show that the most appropriate multidimensional copulas functions to construct the nonlinear multivariate drought index (NMDI) in the JRB, BRB, UWRB, MWRB, LWRB, and WRB are Gumbel, Frank, Frank, Gumbel, Gumbel, and Gumbel, respectively.

(2) Correlation coefficients between the NMDI and single drought index are mostly over 0.7 indicating that the NMDI can reflect the comprehensive meteorological, hydrological and agricultural drought properties simultaneously. This suggests that the copulas can solve the complicated and nonlinear relationship among different drought indices. In addition, the margin-free characteristics are completely preserved by the copulas function when constructing the joint distribution function.

(3) Drought frequency analysis based on the NMDI is consistent with the PAP, SDI, MPDSI and MIDI. Moreover, the NMDI is basically more sensitive to capture more historical recorded drought occurrences, indicating that the NMDI is reliable and superior.

(4) Drought risk shows a spatial variation. For scenario 1 (droughts more likely to happen), the drought risks in the JRB, UWRB, and MWRB are higher. For scenario 2 (droughts less likely to happen), the drought risks in the UWRB and MWRB are higher. This indicates that the likely occurrence drought possibilities in the JRB, UWRB, and MWRB are higher.

Although the WRB is selected as the study area, the constructed NMDI can also be applied in other regions. How to assess the impacts of meteorological, hydrological, and agricultural droughts on society and the economy is the priority of our next study.

In addition, more drought characteristics will be considered for better drought risk assessment.

Acknowledgments

This research is supported by The National Key Research and Development Program of China (2016YFC0400906), National Natural Science Foundation of China (51679189, 51679187, 51647112), Doctor Innovation Foundation of Xi'an University of Technology (310-252071605). Appreciation is extended to the editor and reviewers for their help.

References

- Akaike, H., 1974. A new look at statistical model identification. *IEEE Transactions on Automatic Control* AC19(6), 716-723.
- Cammalleri, C., Micale, F., Vogt, J., 2015. A novel soil moisture-based drought severity index (DSI) combining water deficit magnitude and frequency. *Hydrol. Process.* 30(2), 289-301.
- Cancelliere, A., Salas, J.D., 2004. Drought length properties for periodic-stochastic hydrologic data. *Water Resour. Res.* 40(2), 389-391.
- Caracciolo, D., Istanbuluoglu, E., Noto, L.V., Collins, S.L., 2016. Mechanisms of shrub encroachment into Northern Chihuahuan Desert Grasslands and impacts of climate change investigated using a cellular automata model. *Adv. Water Resour.* 91, 46-62.

- Chang, J., Li, Y., Wang, Y., Yuan, M., 2016. Copula-based drought risk assessment combined with an integrated index in the Wei River Basin, China. *J. Hydrol.* 540, 824-834.
- Chang, J., Wang, Y., Istanbuluoglu, E., Bai, T., Huang, Q., Yang, D., Huang, S., 2014. Impact of climate change and human activities on runoff in the Weihe River Basin, China. *Quatern. Int.* 380-381, 169-179.
- Favre, A., Adlouni, S.E., Perreault, L., Thiémonge, N., Bobée, B., 2004. Multivariate hydrological frequency analysis using copulas. *Water Resour. Res.* 40(1), 290-294.
- Jeong, C., Lee, T., 2015. Copula-based modeling and stochastic simulation of seasonal intermittent streamflows for arid regions. *J. Hydro-environ Res.* 9(4), 604-613.
- Hao, Z., Aghakouchak, A., 2013. Multivariate Standardized Drought Index: A parametric multi-index model. *Adv. Water Resour.* 57(9), 12-18.
- Hao, Z., Hao, F., Singh, V.P., 2016. A general framework for multivariate multi-index drought prediction based on Multivariate Ensemble Streamflow Prediction (MESP). *J. Hydrol.* 539, 1-10.
- Hao, Z., Singh, V.P., 2015. Drought characterization from a multivariate perspective: A review. *J. Hydrol.* 527, 668-678.
- Huang, S., Chang, J., Huang, Q., Chen, Y., 2014. Spatio-temporal Changes and Frequency Analysis of Drought in the Wei River Basin, China. *Water Resour. Manag.* 28(10), 3095-3110.

- Huang, S., Chang, J., Leng, G., Huang, Q., 2015. Integrated index for drought assessment based on variable fuzzy set theory: A case study in the Yellow River basin, China. *J. Hydrol.* 527, 608-618.
- Kao, S. C., Govindaraju, S.G., 2010. A copula-based joint deficit index for droughts. *J. Hydrol.* 380, 121-134.
- Keyantash, J. A., Dracup, J.A., 2004. An aggregate drought index: Assessing drought severity based on fluctuations in the hydrologic cycle and surface water storage. *Water Resour. Res.* 40(9), 333-341.
- Li, X., Waddington, S.R., Dixon, J., Joshi, A.K., Vicente, M.C.D., 2011. The relative importance of drought and other water-related constraints for major food crops in South Asian farming system. *Food Secur.* 3(1), 19-33.
- Ma, M., Song, S., Ren, L., Jiang, S., Song, J., 2013. Multivariate drought characteristics using trivariate Gaussian and Student t copulas. *Hydrol. Process.* 27(8), 1175-1190.
- Ma, M., Ren, L., Singh, V.P., Yuan, F., Jiang, S., 2014. New variants of the palmer drought scheme capable of integrated utility. *J. Hydrol.* 519, 1108-1119.
- Madadgar, S., Moradkhani, H., Garen, D., 2014. Towards improved post-processing of hydrologic forecast ensembles. *Hydrol. Process.* 28(1), 104-122.
- Maity, R., Suman, M., Verma, N.K., 2016. Drought prediction using a wavelet based approach to model the temporal consequences of different types of droughts. *J. Hydrol.* 539, 417-428.
- Meyer, S.J., Hubbard, K.G., Wilhite, D.A., 1991. The relationship of climatic indices

- and variables to corn (maize) yields: a principal components analysis. *Agr. Forest Meteorol.* 55(1-2), 59-84.
- Mishra, A.K., Singh, V.P., 2010. A review of drought concepts. *J. Hydrol.* 391, 202-216.
- Mo, K.C., Lettenmaier, D.P., 2014. Objective drought classification using multiple land surface models. *J. Hydrometeorol.* 15 (3), 990–1010.
- Nalbantis, I., Tsakiris, G., 2009. Assessment of Hydrological Drought Revisited. *Water Resour. Manag.* 23(5), 881-897.
- Nam, W.H., Hayes, M.J., Svoboda, M.D., Tadesse, T., Wilhite, D.A., 2015. Drought hazard assessment in the context of climate change for South Korea. *Agr. Water Manage.* 160, 106-117.
- Palmer, W.C., 1965. Meteorological drought. Res. Pap. 45, 58 pp., Weather Bur., U.S. Dep. of Commer., Washington, D. C.
- Rajsekhar, D., Singh, V.P., Mishra, A.K., 2015. Multivariate drought index: An information theory based approach for integrated drought assessment. *J. Hydrol.* 526, 164-182.
- Svoboda, M., LeComte, D., Hayes, M., Heim, R., Gleason, K., Angel, J., Stephens, S., 2002. The drought monitor. *Bul. Am. Met. Soc.* 83 (8).
- Tabari, H., Nikbakht, J., Talaei, P.H., 2013. Hydrological Drought Assessment in Northwestern Iran Based on Streamflow Drought Index (SDI). *Water Resour. Manag.* 27(1), 137-151.
- Wang, J., Li, Y., Ren, Y., Liu, Y., 2013. Comparison among Several Drought Indices

in the Yellow River Valley. *Journal of natural resources* 8, 1137-1349 (in Chinese).

Waseem, M., Ajmal, M., Kim, T.W., 2015. Development of a new composite drought index for multivariate drought assessment. *J. Hydrol.* 527, 30-37.

Wilhite, D.A., 2001. *Drought: A global Assessment*. Routledge.

Xu, K., Yang, D., Xu, X., Lei, H., 2015. Copula based drought frequency analysis considering the spatio-temporal variability in Southwest China. *J. Hydrol.* 527, 630-640.

Yang, J., Wang, Y., Chang, J., Yao, J., Huang, Q., 2016. Integrated assessment for hydrometeorological drought based on Markov chain model. *Nat. Hazards* 84(2), 1-24.

Zhang, Y., Song, S.B., 2011. Research on Three-dimensional Joint Distribution of Drought Characteristics Based on Archimedean Copulas. *China Rural Water and Hydropower* 1, 65-68 (in Chinese).

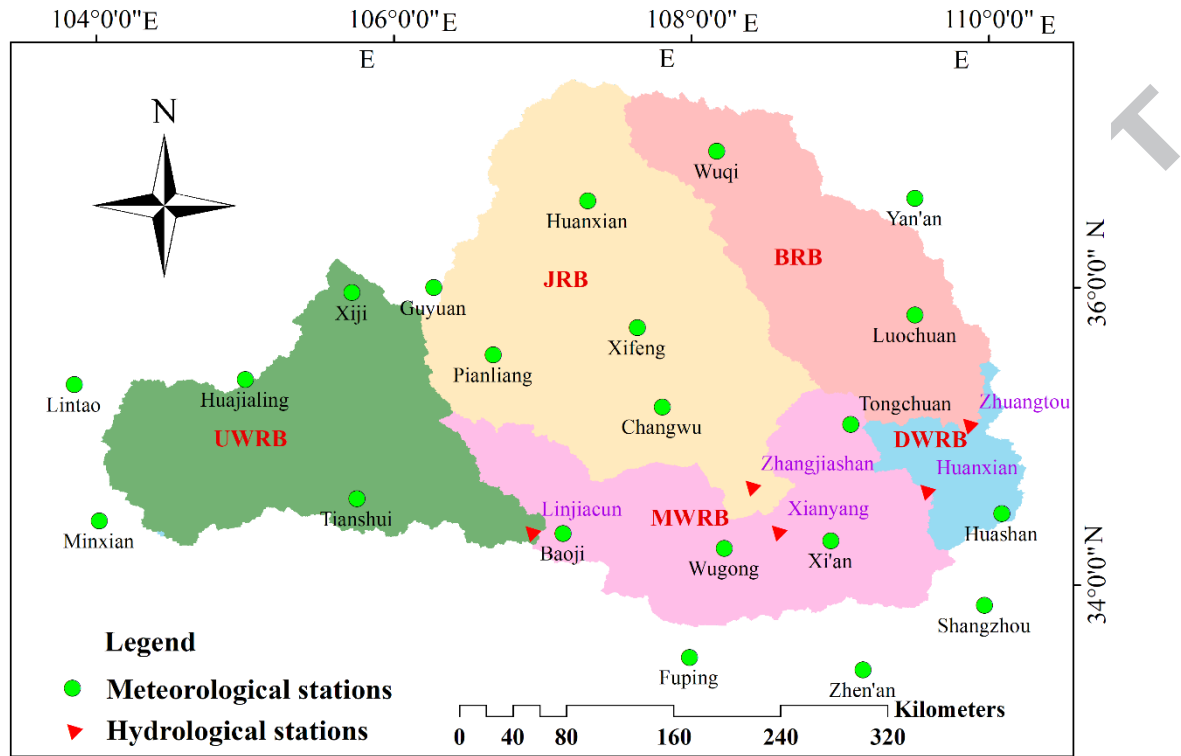


Fig. 1. Meteorological stations and hydrological stations in the Wei River Basin

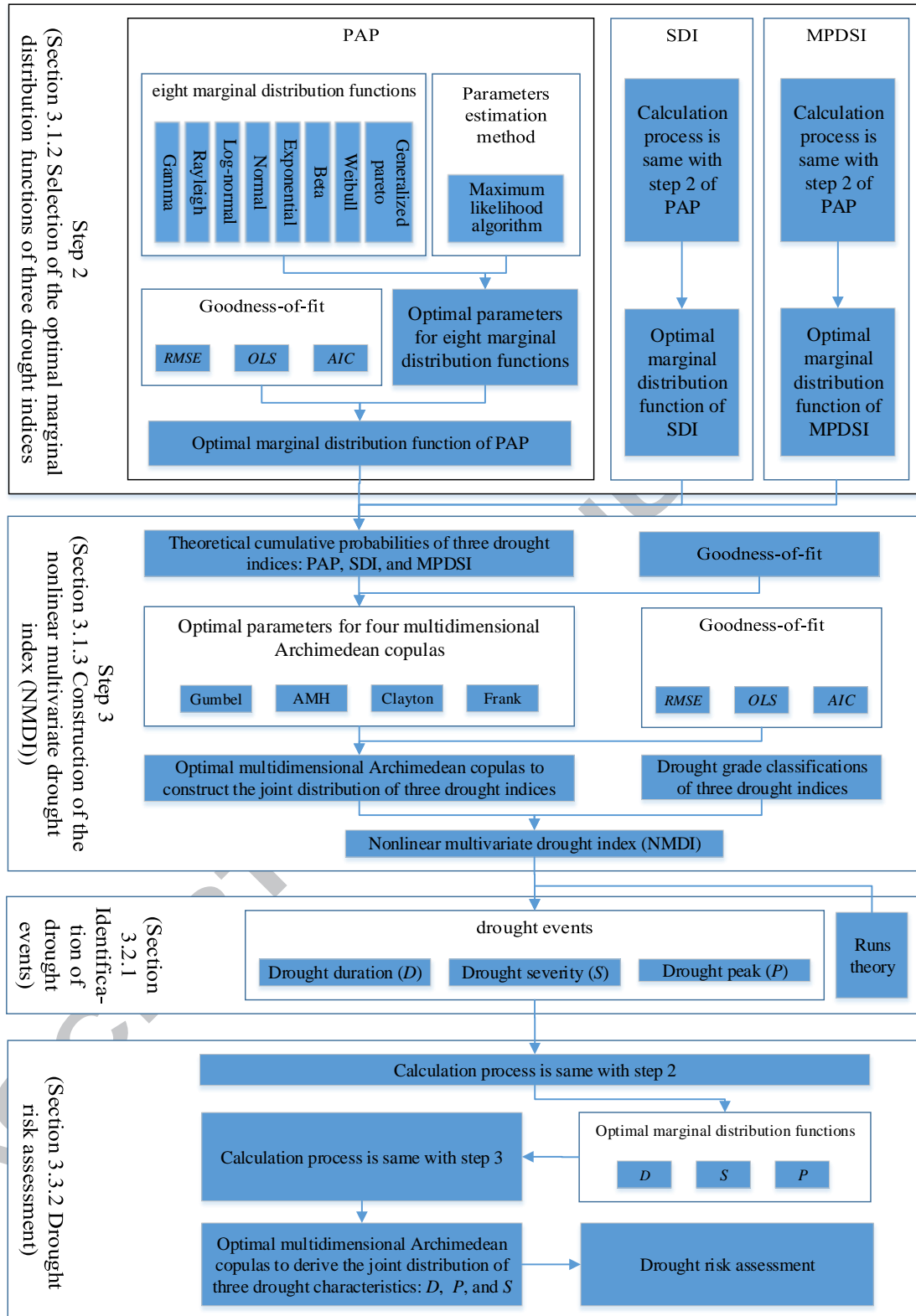


Fig. 2. Main flowchart of construction of the NMDI and drought risk assessment

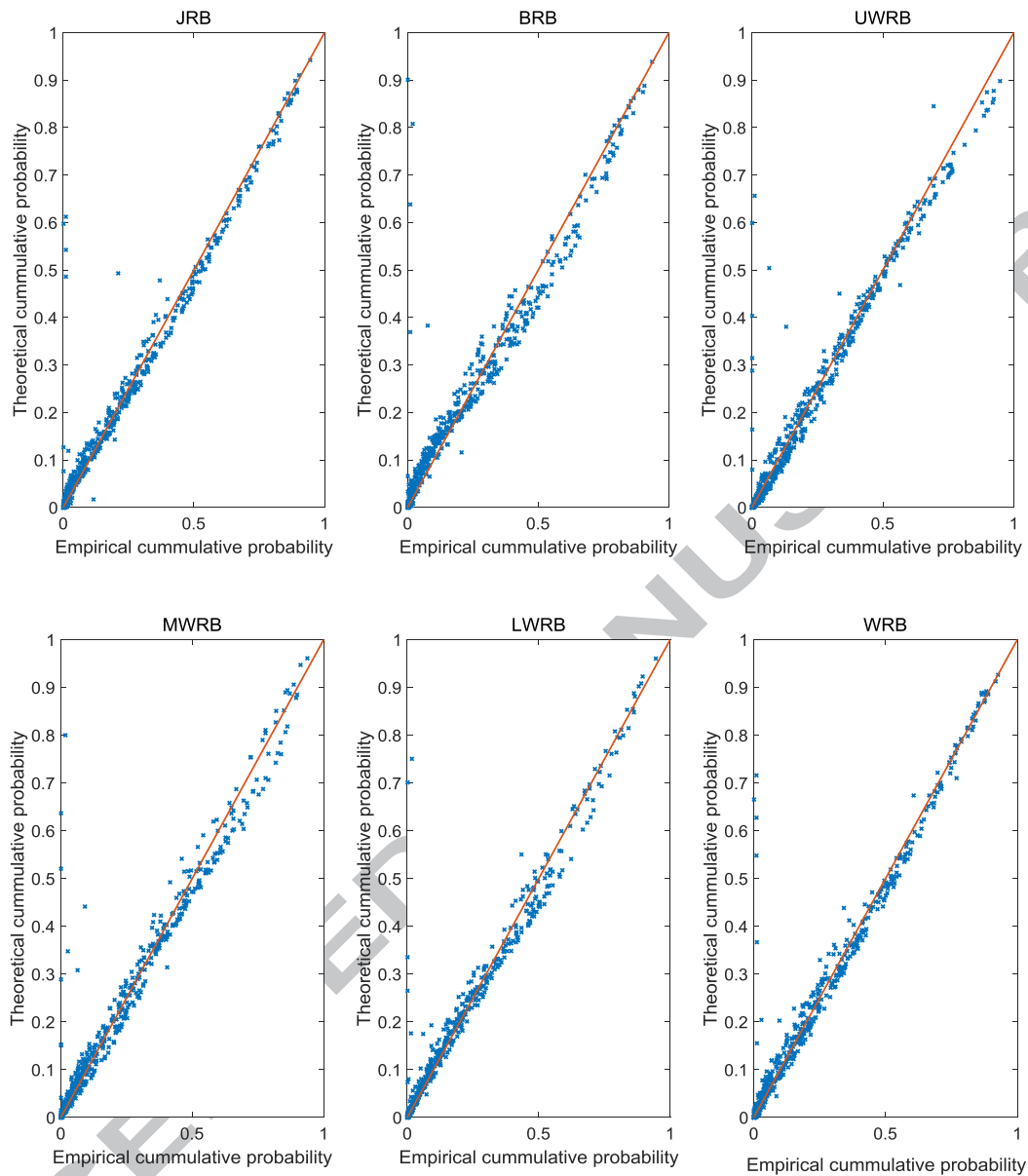


Fig. 3. Comparisons between 3-dimensional empirical and theoretical joint cumulative probability of three drought indices

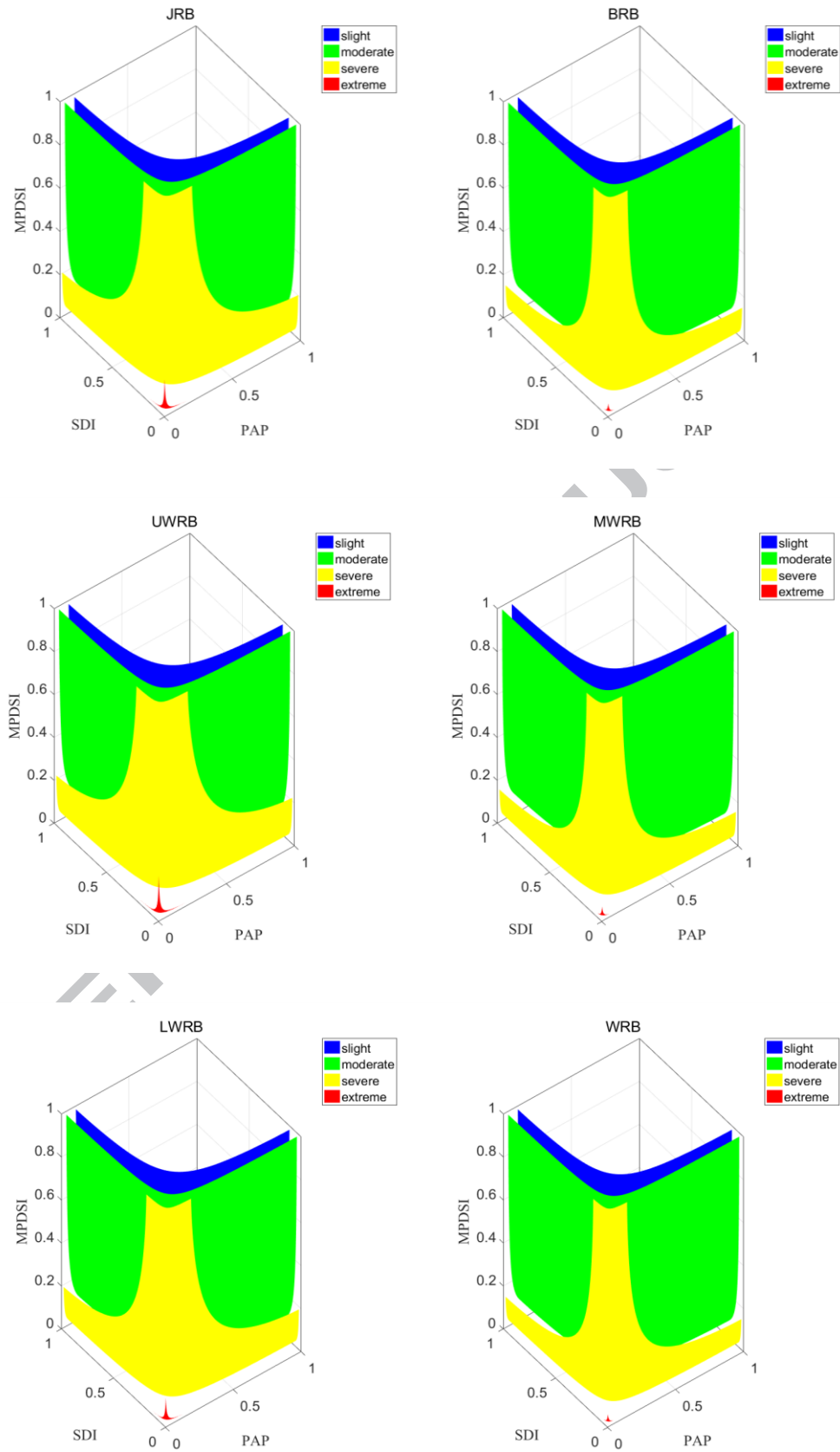


Fig. 4. Spatial diagram of drought grade classifications of NMDI

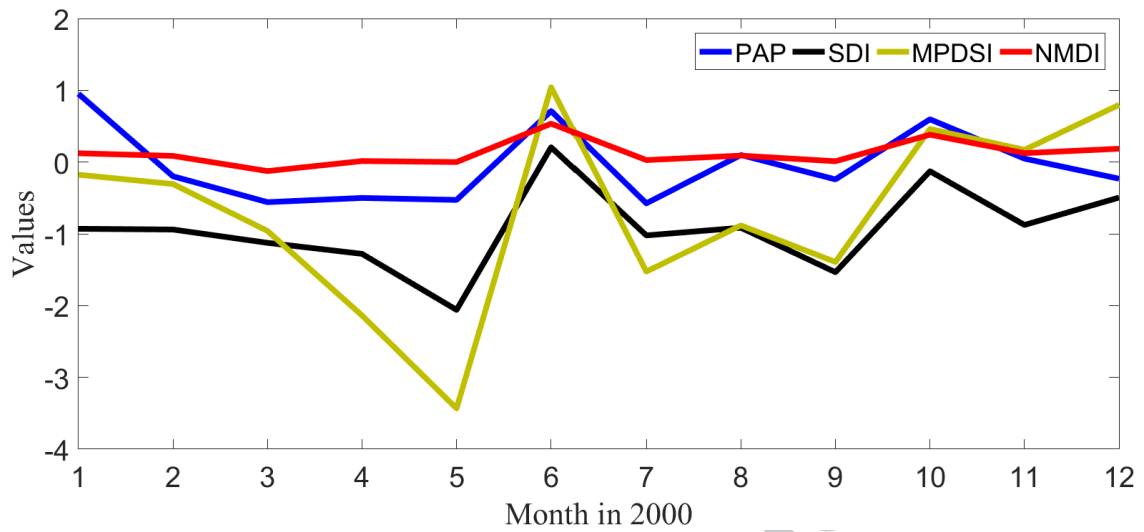


Fig. 5. Comparison between the NMDI, PAP, SDI and MPDSI of the WRB in 2000.

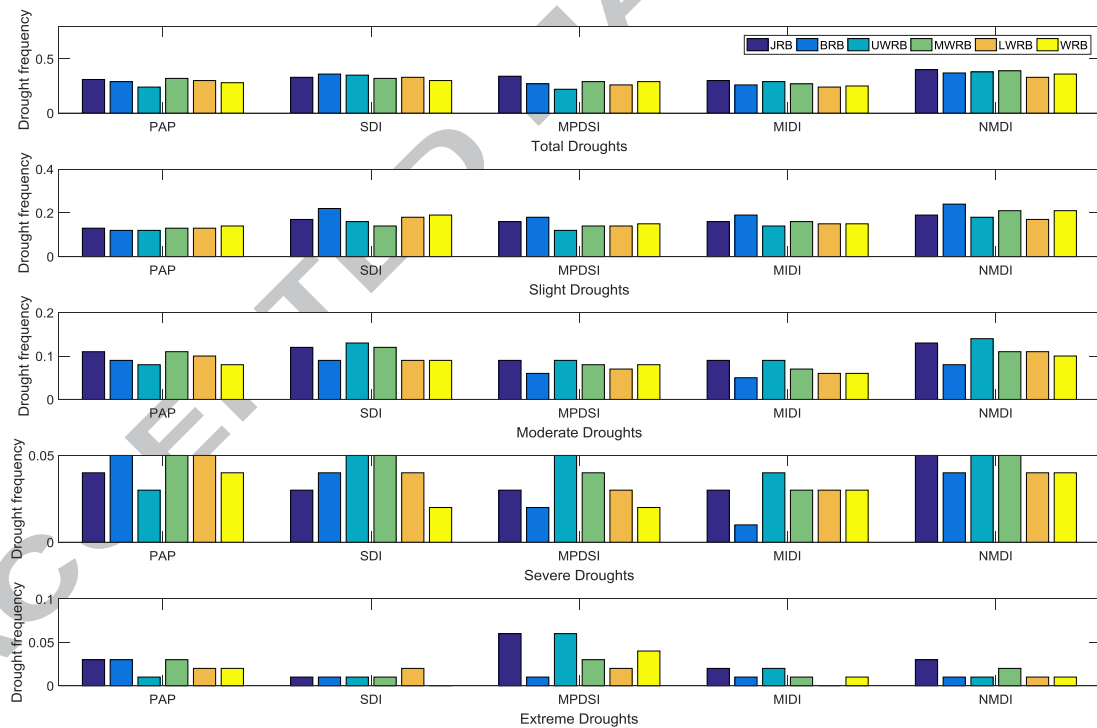


Fig. 6. Drought frequency comparison analysis among different drought indices

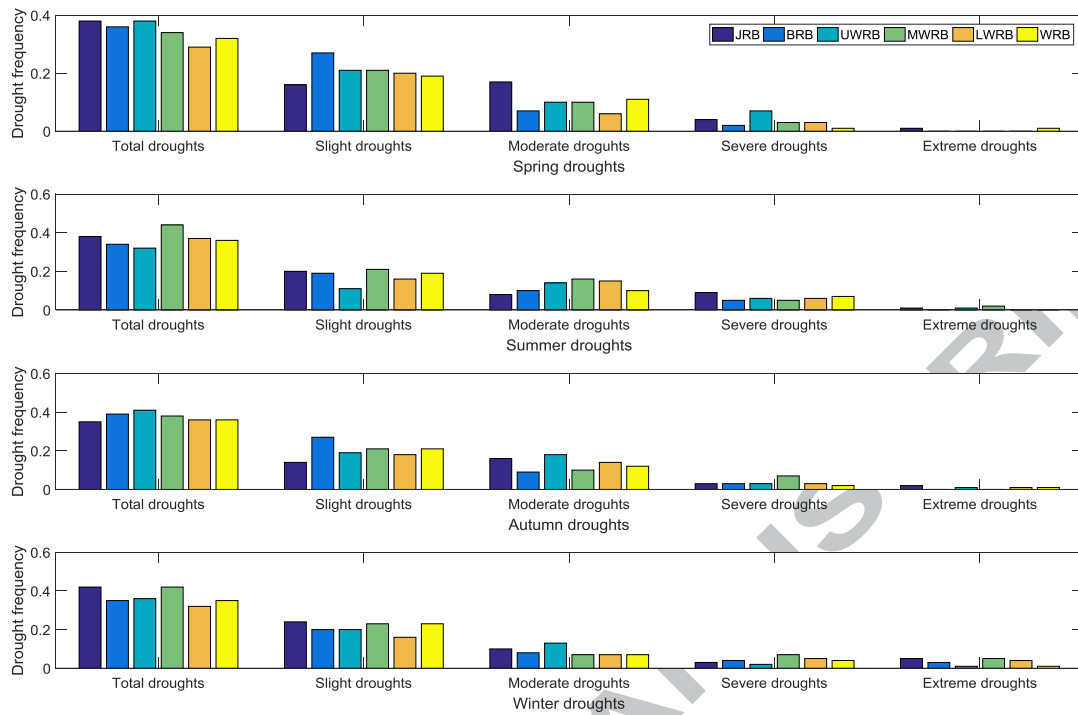


Fig. 7. Seasonal drought frequency analysis based on the constructed NMDI

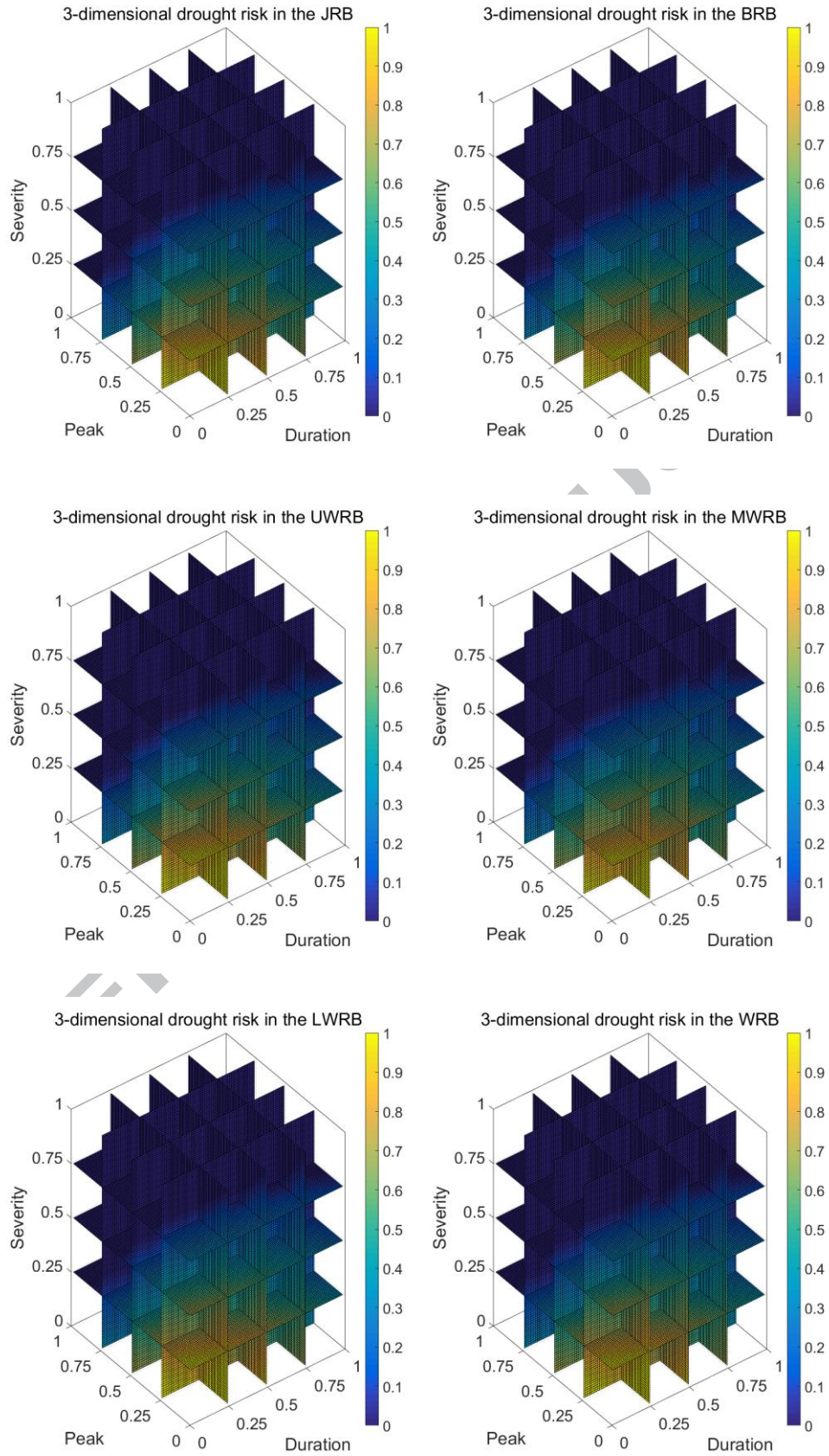


Fig. 8. Slice map of the multivariate drought risk

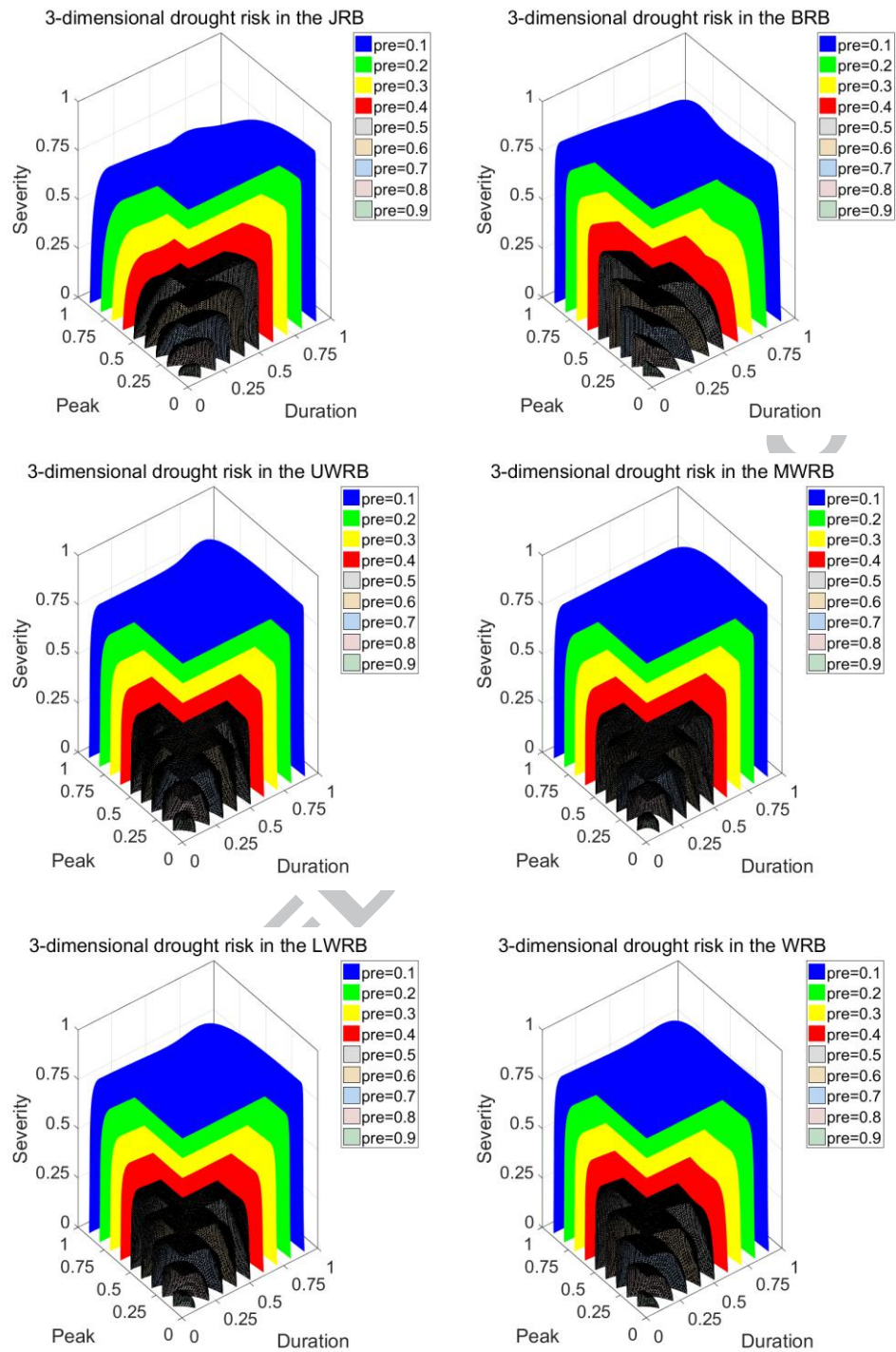


Fig. 9. Contour surface of the multivariate drought risk of the D , P and S

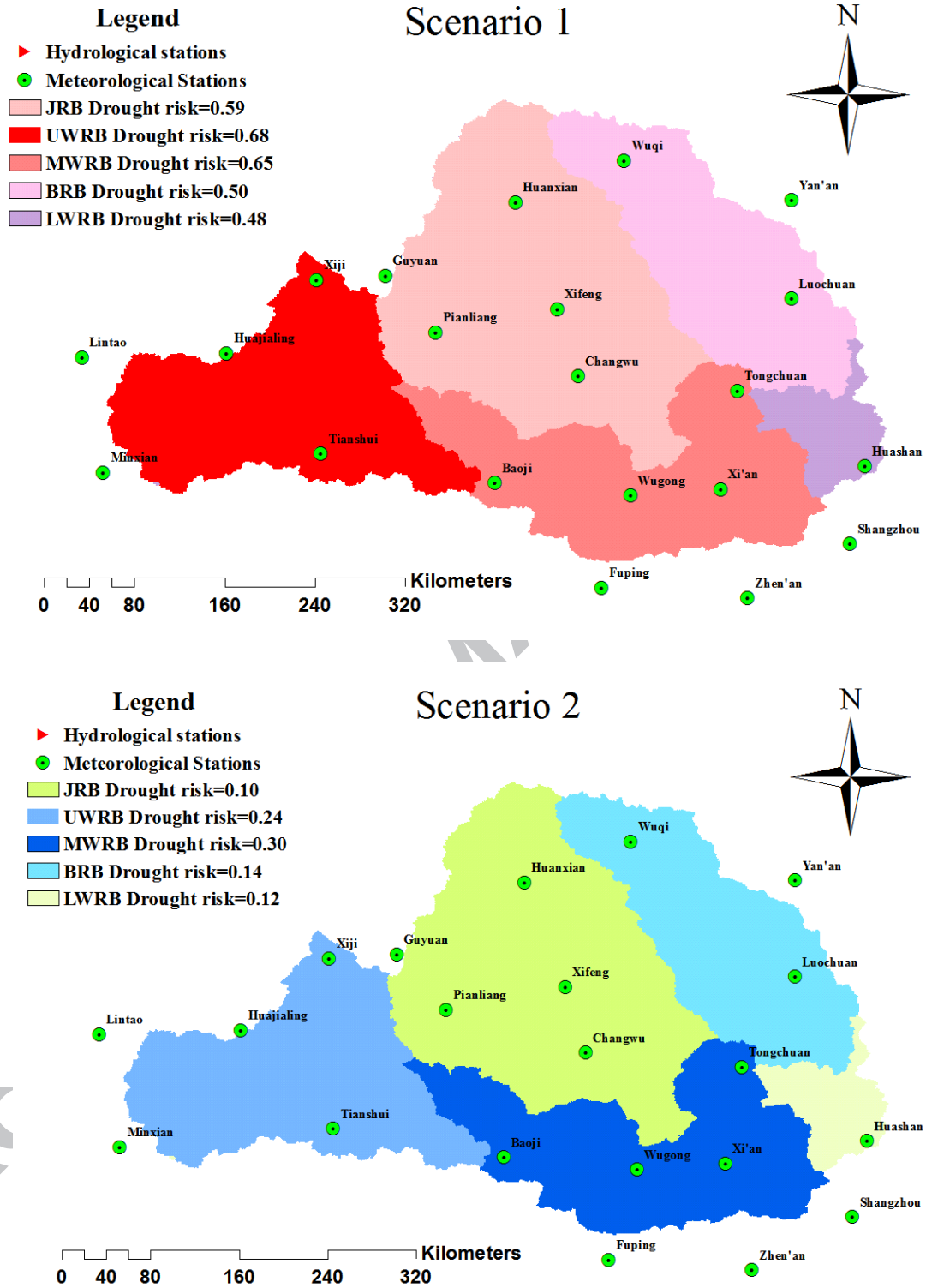


Fig. 10. Drought risks under two scenarios

Table 1 Drought grade classifications of the PAP, SDI, and MPDSI

Drought levels	PAP	SDI	MPDSI
----------------	-----	-----	-------

No drought	$-0.4 < \text{PAP}$	$-0.5 < \text{SDI}$	$-1.0 < \text{MPDSI}$
Slight drought	$-0.6 < \text{PAP} \leq -0.4$	$-1.0 < \text{SDI} \leq -0.5$	$-2.0 < \text{MPDSI} \leq -1.0$
Moderate drought	$-0.8 < \text{PAP} \leq -0.6$	$-1.5 < \text{SDI} \leq -1.0$	$-3.0 < \text{MPDSI} \leq -2.0$
Severe drought	$-0.95 < \text{PAP} \leq -0.8$	$-2.0 < \text{SDI} \leq -1.5$	$-4.0 < \text{MPDSI} \leq -3.0$
Extreme drought	$\text{PAP} \leq -0.95$	$\text{SDI} \leq -2.0$	$\text{MPDSI} \leq -4.0$

ACCEPTED MANUSCRIPT

Table 2 Probability density functions of eight marginal distribution functions

Distribution function	Probability density function	Parameters
Gamma	$f(x, \beta, \alpha) = \frac{\beta^\alpha}{\Gamma(\alpha)} x^{\alpha-1} e^{-\beta x}$	α : shape β : scale
Rayleigh	$f(x) = \frac{x}{\sigma^2} e^{-\frac{x^2}{2\sigma^2}}$	σ^2 : the variance
Log-normal	$f(x) = \frac{1}{x\sigma\sqrt{2\pi}} e^{-\frac{(\ln x - u)^2}{2\sigma^2}}$	u : the mean σ^2 : the variance
Normal	$f(x) = \frac{1}{\sqrt{2\pi}\sigma} e^{-\frac{(x-u)^2}{2\sigma^2}}$	u : the mean σ^2 : the variance
Beta	$f(x) = \frac{1}{B(\alpha, \beta)} x^{\alpha-1} (1-x)^{\beta-1}$	α : shape β : shape
Exponential	$f(x) = \lambda e^{-\lambda x}$	λ : rate
Weibull	$f(x) = \frac{\alpha}{\beta} \left(\frac{x}{\beta}\right)^{\alpha-1} e^{-(x/\beta)^\alpha}$	α : shape β : scale
Generalized pareto	$f(x) = 1 - e^{-\frac{x-u}{\alpha}}$	u : location α : scale

Table 3 Distribution functions of multidimensional Archimedean copulas

Function	Distribution function $C(u, v, w)$	Scope of parameter θ
Gumbel	$e^{-[(-\ln u)^\theta + (-\ln v)^\theta + (-\ln w)^\theta]^{1/\theta}}$	$[1, \infty)$
AMH	$\frac{uvw}{1 - \theta(1-u)(1-v)(1-w)}$	$[-1, 1)$
Clayton	$\max[(u^{-\theta} + v^{-\theta} + w^{-\theta} - 2)^{-1/\theta}, 0]$	$(0, \infty)$
Frank	$-\frac{1}{\theta} \ln \left[1 + \frac{(e^{-\theta u} - 1)(e^{-\theta v} - 1)(e^{-\theta w} - 1)}{(e^{-\theta} - 1)^2} \right]$	$(-\infty, +\infty) \setminus \{0\}$

Table 4 GOF criteria results of the marginal distribution functions and parameters of the PAP in the JRB

Function	Parameters	Three evaluation indices		
		<i>RMSE</i>	<i>OLS</i>	<i>AIC</i>
Gamma	$\alpha = 0.1444$; $\beta = 1.4375$	0.0515	0.0514	-1387.46
Rayleigh	$\sigma^2 = 0.1773$	0.0657	0.0656	-1275.03
Log-normal	$u = -1.9585$; $\sigma^2 = 1.4315$	0.1165	0.1164	-1004.35
Normal	$u = 0.2076$; $\sigma^2 = 0.1408$	0.0466	0.0465	-1434.39
Beta	$\alpha = 0.8814$; $\beta = 2.8188$	0.0724	0.0723	-1227.45
Exponential	$\lambda = 0.2076$	0.0935	0.0934	-1109.53
Weibull	$\alpha = 0.2242$; $\beta = 1.3716$	0.0310	0.0309	-1625.81
Generalized pareto	$u = -0.2263$; $\alpha = 0.2487$;	0.0678	0.0677	-1258.21

Table 5 GOF criteria results of the optimal Archimedean copulas and parameters in the five partitions and the WRB

Partition	Optimal copulas	θ	Three evaluation indices		
			<i>RMSE</i>	<i>OLS</i>	<i>AIC</i>
JRB	Gumbel	1.3674	0.053936	0.053886	-1367.57
	AMH	0.9999	0.075146	0.075077	-1212.02
	Clayton	1.6280	0.059388	0.059333	-1322.41
	Frank	2.4367	0.054676	0.054625	-1361.18
BRB	Gumbel	1.5249	0.070180	0.070115	-1244.09
	AMH	0.9999	0.097572	0.097481	-1089.53
	Clayton	1.8605	0.076430	0.076359	-1204.07
	Frank	3.2059	0.070143	0.070078	-1244.34
UWRB	Gumbel	1.3414	0.057392	0.057339	-1338.44
	AMH	0.9999	0.075655	0.075585	-1208.85
	Clayton	1.7030	0.057264	0.057211	-1339.48
	Frank	2.4204	0.056314	0.056262	-1347.34
MWRB	Gumbel	1.5049	0.062061	0.062004	-1301.76
	AMH	0.9999	0.092397	0.092312	-1115.09
	Clayton	1.9006	0.068971	0.068907	-1252.24
	Frank	3.1469	0.063292	0.063234	-1292.54
LWRB	Gumbel	1.4013	0.054067	0.054016	-1366.44
	AMH	0.9999	0.077505	0.077433	-1197.52
	Clayton	1.6554	0.060591	0.060535	-1313.00
	Frank	2.5651	0.055218	0.055166	-1356.56
WRB	Gumbel	1.5282	0.061905	0.061848	-1302.93
	AMH	0.9999	0.093365	0.093279	-1110.20
	Clayton	1.9663	0.066658	0.066596	-1268.24
	Frank	3.2745	0.061974	0.061917	-1302.41

Table 6 Drought grade classifications of the NMDI

Drought levels	NMDI values	
	JRB	BRB
No drought	$0.10021 < \text{NMDI}$	$0.10879 < \text{NMDI}$
Slight drought	$0.02976 < \text{NMDI} \leq 0.10021$	$0.02166 < \text{NMDI} \leq 0.10879$
Moderate drought	$0.00476 < \text{NMDI} \leq 0.02976$	$0.00139 < \text{NMDI} \leq 0.02166$
Severe drought	$0.00023 < \text{NMDI} \leq 0.00476$	$0.00004 < \text{NMDI} \leq 0.00139$
Extreme drought	$\text{NMDI} \leq 0.00023$	$\text{NMDI} \leq 0.00004$
Drought levels	NMDI values	
	UWRB	MWRB
No drought	$0.09433 < \text{NMDI}$	$0.10172 < \text{NMDI}$
Slight drought	$0.02239 < \text{NMDI} \leq 0.09433$	$0.03019 < \text{NMDI} \leq 0.10172$
Moderate drought	$0.00171 < \text{NMDI} \leq 0.02239$	$0.00518 < \text{NMDI} \leq 0.03019$
Severe drought	$0.00001 < \text{NMDI} \leq 0.00171$	$0.00033 < \text{NMDI} \leq 0.00518$
Extreme drought	$\text{NMDI} \leq 0.00001$	$\text{NMDI} \leq 0.00033$
Drought levels	NMDI values	
	LWRB	WRB
No drought	$0.08318 < \text{NMDI}$	$0.09521 < \text{NMDI}$
Slight drought	$0.02184 < \text{NMDI} \leq 0.08318$	$0.02098 < \text{NMDI} \leq 0.09521$
Moderate drought	$0.00285 < \text{NMDI} \leq 0.02184$	$0.00167 < \text{NMDI} \leq 0.02098$
Severe drought	$0.00009 < \text{NMDI} \leq 0.00285$	$0.000002 < \text{NMDI} \leq 0.00167$
Extreme drought	$\text{NMDI} \leq 0.00009$	$\text{NMDI} \leq 0.000002$

Table 7 Correlation analyses among different drought indices

Project	Correlation coefficient in each partition					
	JRB	BRB	UWRB	MWRB	LWRB	WRB
PAP-SDI	0.3889	0.3706	0.3433	0.3987	0.3590	0.4264
PAP-MPDSI	0.4043	0.3282	0.4366	0.3395	0.2747	0.4031
SDI-MPDSI	0.4729	0.5470	0.5648	0.5756	0.4679	0.6259
PAP-NMDI	0.7292	0.7250	0.7411	0.7348	0.7146	0.7557
SDI-NMDI	0.7284	0.7381	0.7184	0.7614	0.7157	0.7562
MPDSI-NMDI	0.7192	0.7043	0.7353	0.6910	0.6546	0.7335

Table 8 Captured drought events based on the PAP, SDI, MPDSI, MIDI, and NMDI

Recorded severe or extreme droughts		Drought indices				
Years	Season	PAP	SDI	MPDSI	MIDI	NMDI
1978	Spring		√			√
1980	Spring		√	√	√	√
	Summer					
1995	Spring	√	√	√	√	√
	Summer		√	√	√	√
1997	Summer	√	√	√	√	√
2000	Spring	√	√	√	√	√
	Summer		√	√	√	√

Table 9 Drought peak, severity, and duration corresponding to drought events

Partition	JRB	BRB	UWRB	MWRB	LWRB	WRB
Drought number	90	98	80	83	85	83
Maximal drought Duration	11	8	12	17	14	10
Average drought duration	2.32	2.00	2.49	2.57	2.11	2.27
Maximal drought peak	0.1	0.11	0.09	0.1	0.08	0.1
Average drought peak	0.07	0.07	0.07	0.07	0.05	0.06
Maximal drought severity	0.83	0.79	0.89	1.5	0.86	0.79
Average drought severity	0.15	0.14	0.16	0.16	0.11	0.13

Table 10 GOF criteria results of the optimal 3-dimensional copulas and parametersfor drought D , P , and S

Partition	Optimal copulas	θ	Three evaluation indices		
			<i>RMSE</i>	<i>OLS</i>	<i>AIC</i>
JRB	Clayton	6.7133	0.0796	0.0791	-195.8577
	AMH	0.9999	0.1410	0.1402	-151.1629
	Gumbel	3.1731	0.0718	0.0714	-203.8990
	Frank	9.5538	0.0742	0.0738	-201.3514
BRB	Clayton	4.1088	0.0975	0.0970	-196.1692
	AMH	0.9999	0.1280	0.1274	-172.9614
	Gumbel	2.1588	0.0810	0.0806	-211.9715
	Frank	6.3199	0.0807	0.0803	-212.2266
UWRB	Clayton	3.8418	0.0959	0.0953	-160.8731
	AMH	0.9999	0.1444	0.1435	-132.4557
	Gumbel	2.6040	0.0972	0.0966	-159.9585
	Frank	7.6571	0.0930	0.0924	-163.0616
MWRB	Clayton	10.9999	0.1029	0.1023	-161.9079
	AMH	0.9999	0.1779	0.1768	-122.4745
	Gumbel	6.4123	0.1026	0.1019	-162.1785
	Frank	10.0001	0.1042	0.1035	-161.0593
LWRB	Clayton	6.3571	0.0998	0.0992	-168.1541
	AMH	0.9999	0.1380	0.1372	-144.1997
	Gumbel	2.4496	0.0950	0.0944	-171.8113
	Frank	7.8699	0.0937	0.0932	-172.7990
WRB	Clayton	3.6423	0.0932	0.0927	-169.0603
	AMH	0.9999	0.1229	0.1222	-149.1216
	Gumbel	2.0402	0.0873	0.0867	-173.8116
	Frank	6.0494	0.0850	0.0845	-175.6830

1. A reliable nonlinear multivariate drought index (NMDI) was constructed.
2. Copulas can better reflect the nonlinear relationship among multiple drought indices when constructing a new composite drought index than linear combination, principal component analysis, and weight method.
3. Drought event including three drought characteristics: duration, peak, and severity was redefined with the NMDI.
4. Multivariate drought risk was fully assessed.
5. Partitions where had higher drought risk were found.